Journal of Advanced Marine Engineering and Technology, Vol. 48, No. 5, pp. 324~330, 2024
J. Advanced Marine Engineering and Technology (JAMET)
https://doi.org/10.5916/jamet.2024.48.5.324

ISSN 2234-7925 (Print)
ISSN 2765-4796 (Online)
Original Paper

Research for implementation of PANS model based on open source code

Gisu Song† · Sungwook Lee[1]

(Received October 10, 2024 ; Revised October 15, 2024 ; Accepted October 22, 2024)

Abstract: Several Hybrid RANS/LES methods which combine advantages of RANS and LES(or DNS) has been proposed. These methods can be very practical for real engineering problems since the required number of grids can be much less than that of LES(or DNS) and unsteady features of flow can predict more realistic than RANS simulation. In this paper, PANS which is one of Hybrid RANS/LES methods is investigated. To know the capability of PANS, two benchmark problems with different flow characteristics were applied with RANS simulation. First benchmark problem is the flow past a wall mounted square cylinder. It is well known that this flow is naturally unstable due to Karman vortex shedding and has complex flow structures in the wake region. Second benchmark problem is the flow around ship which is chosen as the KCS. The ship is a representative streamlined body, and three dimensional weak flow separation is induced. In this paper, based on these flows, the simulation results from RANS and PANS were compared. And the k-ω turbulence model is applied for RANS and PANS simulations with open source code.

Keywords: PANS(Partially Averaged Navier-Stokes), Hybrid RANS/LES, Ship, Square Cylinder, Open Source Code

1. Introduction

As computational fluid dynamics (CFD) has been widely applied from the 1980s, in various CFD methodologies, the Reynolds-Averaged Navier-Stokes (RANS) method with turbulence model has been mainly used to actual engineering problems. This method requires relatively low calculation cost and time comparing to the other methodologies. However, the results from RANS simulation are depending on the turbulence model which is the mathematical modeling of unsteady behavior of eddy in turbulent flow. In addition, the accuracy of prediction for the flow with separation is a well-known shortcoming. In the other hands, other method such as Direct Numerical Simulation (DNS) has begun to be used to describe the turbulent flow from the 1990s. Because DNS shows very accurate computational results by directly resolving the smallest scale of turbulence, it is very useful to understand the complex physical phenomenon of turbulence. But it requires too much computational cost and time, so it is practically impossible to apply for engineering problems. And Large Eddy Simulation (LES) has been also applied to simulate a turbulent flow. In LES, the small scale eddy is modeled based on the generality of turbulence, whereas large scale eddy is directly resolved. Since LES directly resolves eddies of important size in the turbulent flow field, more accurate results can be obtained compared to RANS. However, in order to accurately simulate a high Reynolds number of turbulent flow fields, an isotropic grid and dense grid resolution are required at near wall. So LES also still requires a lot of computational cost and time.

As an alternative, the Hybrid RANS/LES method has been developed to improve the practicality and accuracy by combining the advantages of RANS and LES (or DNS). This method was proposed to compensate for the shortcomings of LES (or DNS), which requires a dense grid system inside the boundary layer near the wall, and the shortcomings of the RANS method, which does not accurately predict turbulence behavior in flow separation region. In the 2000s, various hybrid RANS/LES methods, for example, Detached Eddy Simulation (DES) **[1]**, PANS **[2]**, and Partially Integrated Transport Model (PITM) **[3]** have been proposed by many researchers. In particular, these methods have been widely applied to many engineering flows and validated to simulate the characteristics of the actual flow field at a relatively low cost.

In this study, the PANS method was applied to simulate

† Corresponding Author (ORCID: http://orcid.org/0000-0002-5424-4794): Professor, Division of naval Architecture and Ocean Systems Engineering, National Maritime & Ocean University, 727, Taejong-ro, Yeongdo-gu, Busan 49112, Korea, E-mail: gisu.song@kmou.ac.kr, Tel: +82-51-410-4307

1 Professor, Division of naval Architecture and Ocean Systems Engineering, National Maritime & Ocean University, E-mail: swlee@kmou.ac.kr, Tel: +82-51-410-4303

turbulent flows with bluff body and streamlined body. The obtained results were compared to those from traditional RANS method. These two methods were applied to two different target flows. At first, the flow around a square cantilever (height/width>4) is chosen as an example of massive separation flow. It is well known that this flow has unsteady characteristics due to periodic vortex shedding and it is very similar to the flow past a two-dimensional square cylinder **[4]-[6]**. In contrast, the flow with weak flow separation is chosen. As well known, the ship is a representative streamlined body and the hull form consists of curved surface. Therefore, the massive separation is not provided but the weak flow separation such as bilge vortex is observed in general. In this study, the KCS (KRISO Container Ship) hull form was selected for numerical simulation with PANS model **[7]**.

2. Numerical set-up

In this chapter, the governing equations of RANS and PANS are presented and compared.

2.1 Governing Equations of RANS

In RANS method, instantaneous velocity field is decomposed into time averaged component, U_i and fluctuation component u_i like **Equation (1)**.

$$V_i = U_i + u_i \tag{1}$$

It is well known that the governing **Equation (2)** and **(3)** for the RANS in incompressible flow are as follows;

Continuity equation:

$$\frac{\partial U_i}{\partial x_i} = 0 \tag{2}$$

Momentum equation:

$$\frac{\partial U_i}{\partial t} + U_j \frac{\partial U_i}{\partial x_j} = -\frac{1}{\rho}\frac{\partial P}{\partial x_i} + \frac{\partial}{\partial x_i}\left(2\nu S_{ij} - \tau_{ij}\right) \tag{3}$$

To model the unknown Reynolds stress τ_{ij}, various turbulence models were suggested. In this work, we selected the k-ω turbulence model since it provides better performance than those of RANS simulation **[8][9]**. This means that unsteady simulation is more appropriate than steady simulation in the fluctuating flow associated with massive separation.

Model equations are shown in **Equation (4)** and **(5)**.

$$\frac{\partial k}{\partial t} + \frac{\partial}{\partial x_j}\left(U_j k - (\nu + \sigma^* \nu_t)\frac{\partial k}{\partial x_j}\right) = P - \beta^* k\omega \tag{4}$$

$$\frac{\partial \omega}{\partial t} + \frac{\partial}{\partial x_j}\left(U_j \omega - (\nu + \sigma \nu_t)\frac{\partial \omega}{\partial x_j}\right) = \alpha\frac{\omega}{k}P - \beta\omega^2 \tag{5}$$

The model constants and the eddy viscosity are given by

$\alpha = \frac{5}{9}$, $\beta = \frac{3}{40}$, $\beta^* = \frac{9}{100}$, $\sigma^* = 0.5$, $\sigma = 0.5$, and $\nu_t = \frac{k}{\omega}$

Typical boundary conditions at the wall are specified as

$$k = 0, \omega = \frac{60\upsilon}{\beta(y_1)^2}$$

where $y_1$is the physical distance of the first grid point away from the wall.

2.2 Governing Equations of PANS

In PANS method, the instantaneous velocity field is decomposed into resolved velocity field, U_i and unresolved velocity field, u_i like **Equation (6)**. The expression of equation is same to **Equation (1)** but the physical and mathematical meaning is different.

$$V_i = U_i + u_i \tag{6}$$

The PANS in incompressible flow are as follows;

Continuity equation:

$$\frac{\partial U_i}{\partial x_i} = 0 \tag{7}$$

Momentum equation:

$$\frac{\partial U_i}{\partial t} + U_j \frac{\partial U_i}{\partial x_j} = -\frac{1}{\rho}\frac{\partial P}{\partial x_i} + \frac{\partial}{\partial x_i}\left(2\nu S_{ij} - \tau_{ij}\right) \tag{8}$$

To make the closed system on these equations, additional equations are also necessary and presented in **Equation (9)** and **(10)**.

$$\frac{\partial k_u}{\partial t} + \frac{\partial}{\partial x_j}\left(U_j k_u - (\nu + \sigma_{ku}\nu_u)\frac{\partial k_u}{\partial x_j}\right) = P_u - \beta^* k_u \omega_u \tag{9}$$

$$\frac{\partial \omega_u}{\partial t} + \frac{\partial}{\partial x_j}\left(U_j \omega_u - (\nu + \sigma_u \nu_u)\frac{\partial \omega_u}{\partial x_j}\right) = \alpha\frac{\omega_u}{k_u}P_u - \bar{\beta}{\omega_u}^2 \tag{10}$$

Where , $\bar{\beta} = \left(\alpha\beta^* + f_k(\beta - \alpha\beta^*)\right)$, the model constants and the eddy viscosity are given by

$\alpha = \frac{5}{9}$, $\beta = \frac{3}{40}, \beta^* = \frac{9}{100}$, $\sigma_{ku} = 0.5, \sigma_u = 2.0$, and $\nu_u = \frac{k_u}{\omega_u}$.

As shown in **Equation (9)** and **(10)**, basic formulations are almost

similar except for the model coefficient, β^* comparing to **Equation (4)** and **(5)**. As shown, **Equation (11)**, this coefficient is defined by control parameter, f_k which means the ratio of unresolved to total turbulent quantity.

$$f_k = \frac{k_u}{k} \tag{11}$$

Where k is turbulent kinetic energy and subscript u means unresolved quantities which can be expressed in modeled equations of k_u. Since PANS **[2]** has been suggested, many researchers have been investigated how to decide the control parameter**[10][11]**. In this study, the control parameter, f_k is defined as a constant, 0.5 for a fundamental comparison of two methodologies.

3. Computational Detail

3.1 Target Flow 1

As written previously, the flow past a wall mounted square cylinder is defined as the target flow 1 and this flow have been studied by experiments **[4][5]**. It is well known that this flow show massive flow separation at corner of a square cylinder. The computational domain is shown in **Figure 1**, and designed based on the experimental study. The Reynolds number (Re_D) based on the width of the square cylinder (D) and the free stream velocity (U_{Ref}) is 11,540. The boundary condition is given in **Figure 2**. Periodic boundary condition was designated on two sides in spanwise direction. The Neumann condition was adopted for the outflow boundary. At all the surface boundaries including a wall mounted square cylinder and bottom surface, no slip condition was imposed, respectively. In inflow boundary, the velocity was defined as a Dirichlet condition. At top, the slip condition was given with same velocity with inflow boundary. The grid system was presented in **Figure 3**, carried out in previous study**[6]**. Total number of grid is about 400,000. The minimum Δz^+ at the center of the top surface of the building is 1.71.

3.2 Target flow 2

The second target flow was defined as the flow around ship. Especially, the KCS is a famous benchmark hull-form for a numerical study, experimental data were also released **[12]**. The main particulars and geometry are given in **Figure 4** and **Table 1**, respectively. The simulation was carried out in model scale.

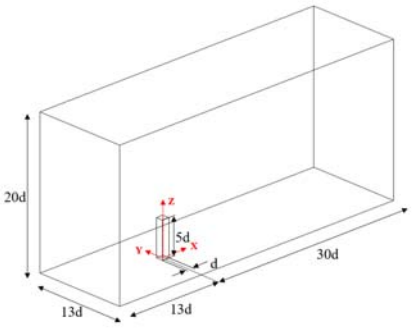

Figure 1: Computational domain for the target flow 1

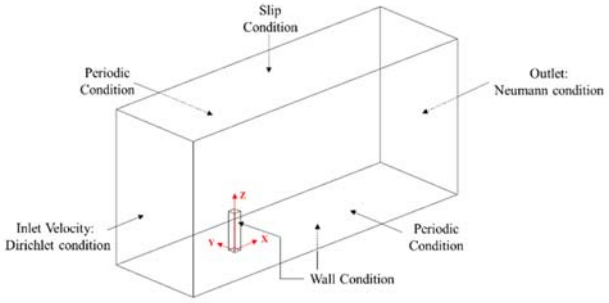

Figure 2: Boundary condition for the target flow 1

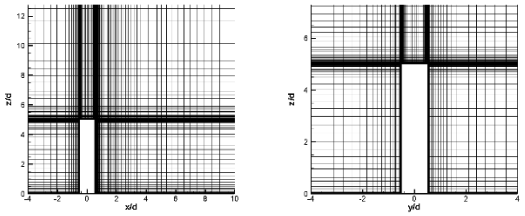

Figure 3: Grid system for the target flow 1

Figure 4: KCS hull geometry

Table 1: Specifications for KCS

Description	Name & Unit	Value
Length Between Perpendiculars	LBP [m]	7.2785
Max. Beam of Waterline	B_{WL} [m]	1.0190
Depth	D [m]	0.6013
Draft	d [m]	0.3418
Wetted Surface area w/o rudder	$S_{w/o\ Rudder}$ [m^2]	9.438
Wetted Surface area of rudder	S_{Rudder} [m^2]	0.115
Block coefficient	C_B	0.6505
Model Ship speed	V_M [m/s]	2.19699
Froude Number	F_n	0.260
Reynolds Number	R_n	1.4×10^7

The computational domain and boundary conditions are shown together in **Figure 5.** Since the hull is a symmetrical geometry, the half-body is only considered for saving the computational time and cost. As presented in **Figure 6,** the unstructured grid system was constructed and the total number of cells is about 1,200,000. The validated grid system in previous study **[7]** was adopted.

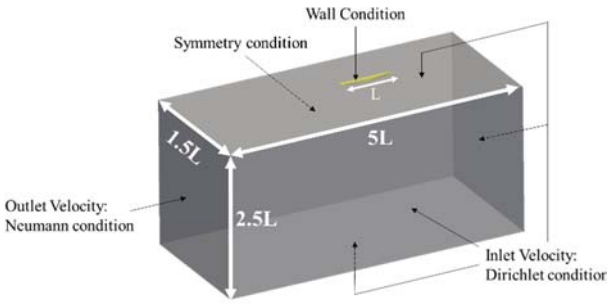

Figure 5: Boundary condition for the target flow 2

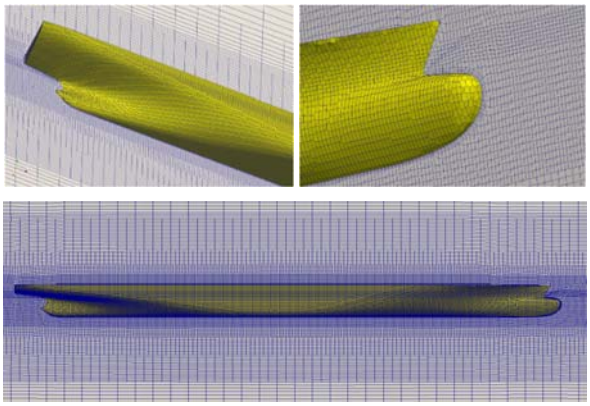

Figure 6: Grid system for the target flow 2

3.3 Code for Numerical Simulation

For numerical simulation, we employed an open source code, called by Open Field Operation and Manipulation (OpenFOAM) which is a one of the well-known incompressible Navier-Stokes solvers. Since this code has been enough verified in many engineering problems, it is thought that there is no doubt about the reliability of the code. The PIMPLE algorithm was implemented for coupling of pressure and velocity, and Crank-Nicholson scheme was used for the temporal discretization. The Gauss linear scheme with second order accuracy was applied for spatial discretization.

4. Results

4.1 Target Flow 1

As already mentioned, a periodic vortex shedding on this flow is the representative characteristics. Therefore, the transient simulation is unavoidable to get the time averaged flow field which was obtained over 150 non-dimensional time. This time period means about 15~16 vortex shedding cycles in this target flow.

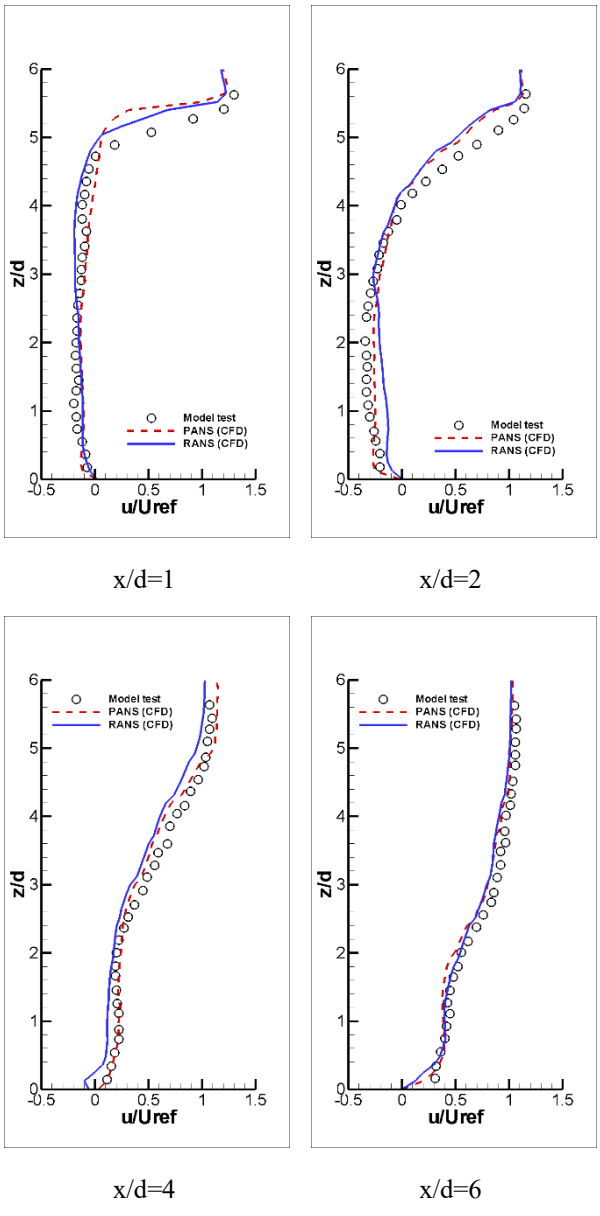

Figure 7: U velocity profile comparison at four locations

The streamwise velocity (U) profiles at 4 streamwise positions (x/d=1, 2, 4, and 6; y/d=0) are compared in **Figure 7**. In this wake region, the velocity profiles from RANS model and PANS are similar each other, but those from PANS shows better agreement

with experimental data for the region on z/d<3. The vertical velocity (W) profiles at the center plane (y/d=0) are given in **Figure 8**. We again see that the velocity profiles from RANS and PANS are similar. But PANS shows better performance in the region on z/d<3. This target flow is naturally unstable due to a large scale flow separation. The flow unsteadiness is dominantly induced by the Karman vortex shedding as explained by previous studies. It is also known that the oscillating flow pattern at the half height plane of a long wall mounted square cylinder is very similar to that of the flow around a two-dimensional square cylinder **[4]-[6]**.

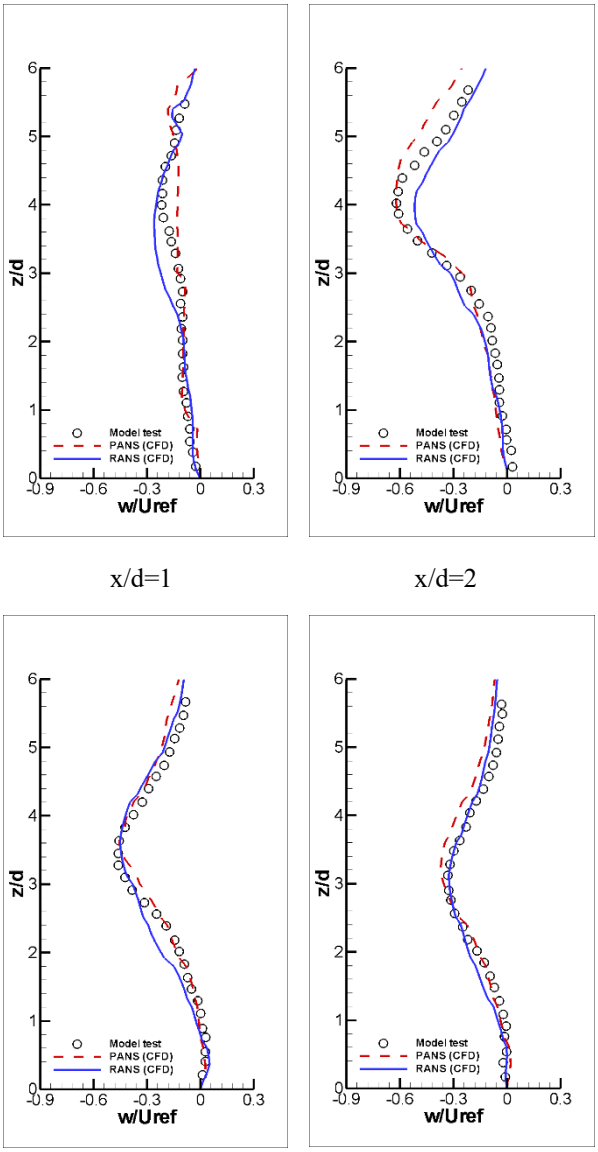

Figure 8: W velocity profile comparison at four locations

To examine the predictability of the flow unsteadiness in two different methods, **Figure 9** shows the vorticity with respect to Y direction distribution extracted at different 4 positions (z/d=1, z/d=2, z/d=3,and z/d=4). The unsteadiness of flow is clearly shown in both simulations and the massive flow separation is observed in 3 positions (z/d=1, z/d=2, and z/d=3). From **Figure 9**, it is known that vortices with small scale are described in PANS model.

To compare the turbulence flow structure, Q-criteria is shown in **Figure 10**. In both simulations, the horseshoe vortices in front of the wall mounted square cylinder was observed similarly. But the flow structures behind the obstacle is more realistically examined in PANS simulation. This shows that the PANS has advantages to simulate the turbulence flow field with massive separation.

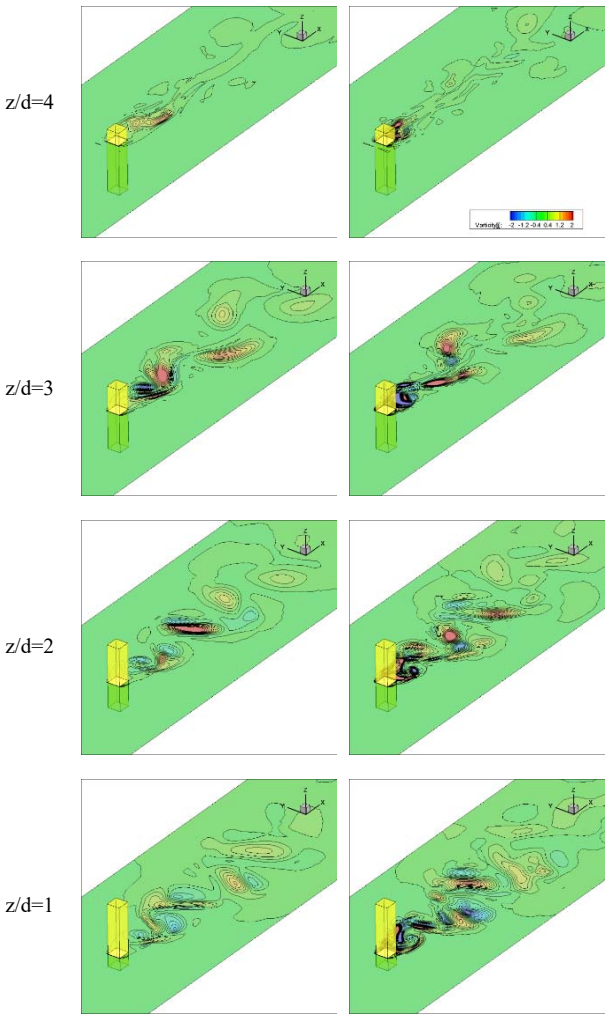

Figure 9: Vorticity distribution in 4 locations of different height

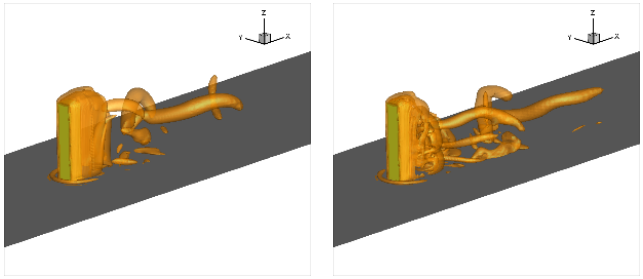

(A) RANS (B) PANS

Figure 10: Q Criteria of numerical simulations (Q=0.5)

4.2 Target Flow 2

In contrast to previous section, the ship is a representative example of the streamlined body. In streamlined body, the massive separation of flow is generally not observed. Of course two pair of bilge vortex is shown in the wake region behind a ship, but it is directly affected by ship type such as a tanker, container, and LNG carrier. Since the ship speed of a container is relatively larger than other types of vessel, the hull form is designed to be more streamlined to reduce the resistance, these bilge vortex is also very weaken.

The total resistance coefficient, C_{TM} is compared in **Table 2**. The results from both simulations showed a similar value and within 1.0% difference. But RANS is slightly agreed well to that of model test rather than PANS.

Table 2: Resistance of KCS in calm sea condition

Description	C_{TM}	Accuracy
Model test **[12]**	3.711×10^{-3}	100.0%
RANS (present)	3.661×10^{-3}	98.7%
PANS (present)	3.634×10^{-3}	97.9%

The **Figure 11** shows the pressure distribution on a FWD-hull by two methods. As well-known, the resistance is oriented by the summation of pressure and skin friction on the target object in general. Since the total resistance value is similar each other, as shown in **Table 2**, it can be inferred that the pressure distribution on a hull is also similar, regardless of the numerical method. In a container ship, it is well known that the portion of the wave resistance in total resistance is relatively larger than the other ship types for example, tanker, bulker and LNG carrier. Therefore the Kelvin wave around container is clearly observed in general. In both simulations, the predicted Kelvin wave are almost similar, as shown in **Figure 12**.

From results based on the second target flow, the difference between of RANS and PANS is relatively negligible rather than those of first target flow.

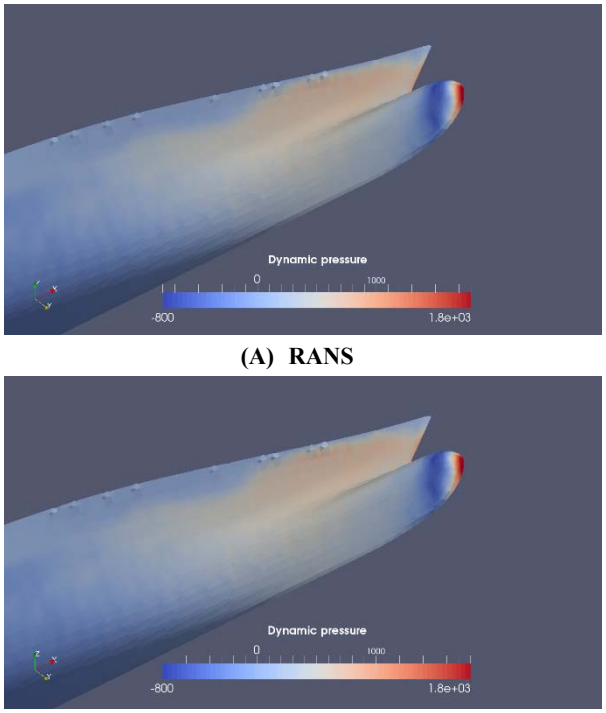

(A) RANS

(B) PANS

Figure 11: Pressure distribution on KCS

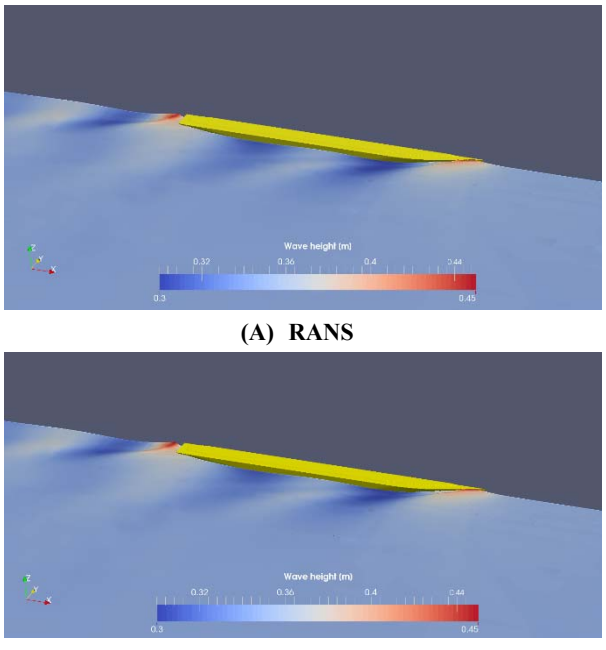

(A) RANS

(B) PANS

Figure 12: Free surface distribution on KCS

4. Conclusion

In this study, we investigated the capability of PANS in two different turbulent flows; the flow past a wall mounted square

cylinder and the flow around KCS. These two flows have contradict characteristics in point of view on fluid mechanics. The first target flow is a representative of the massive flow separation, the second flow is typically considered as streamlined flow.

The PANS method showed better performance to predict the unsteady characteristics of flow than RANS simulation. Especially, instantaneous turbulent flow structures were predicted realistically and the time averaged velocity quantities such as velocity profiles in wake region were agreed well to those of model test. On the other hands, the flow around KCS from PANS was similarly predicted with those of RANS. Although the total resistance coefficient from PANS simulation is 0.8% less than that from RANS simulation, these results showed about 2% difference comparing to the measurement on the model test. In calm water, the difference of Kelvin wave on the free surface or pressure distribution on hull surface between RANS and PANS simulations are almost negligible.

From this study, it is concluded that the PANS method can be a relatively good selection for the numerical simulation of a turbulent flow with massive separation.

Acknowledgement

This work was supported by the Korea Maritime And Ocean University Research Fund in 2021.

Author Contributions

Conceptualization, G.S. Song; Methodology, G.S. Song; Software, G.S. Song, S.W. Lee; Validation, G.S. Song, S.W. Lee; Resources, S.W. Lee; Data Curation, G.S. Song; Writing—Original Draft Preparation, G.S. Song; Writing—Review & Editing, G.S. Song; Visualization, G.S. Song; Supervision, G.S. Song; Project Administration, G.S. Song; Funding Acquisition, G.S. Song.

References

[1] P. R. Spalart, W. H. Jou, M. Strelets, and S. R. Allmaras, “Comments on the feasibility of LES for wings and on a hybrid RANS/LES approach,” Advances in DNS/LES: First AFOSR International Conference on DNS/LES, 1997.

[2] S. S. Girimaji, R. Sreenivasan, and E. Jeong, “PANS turbulence model for seamless transition between RANS and LES: Fixed-point analysis and preliminary results,” Proceedings of ASME FEDSM’03 2003 4th ASME-JSME Joint Fluids Engineering Conference, 2003.

[3] R. Schiestel and A. Dejoan, “Towards a new partially integrated transport model for coarse grid and unsteady turbulent flow simulations,” Theoretical Computational Fluid Dynamics, vol. 18, pp. 443-468, 2005.

[4] H. F. Wang, Y. Zhou, C. K. Chan, W. O. Wong, and K. S. Lam, “Flow structure around a finite-length square prism,” Proceedings of the 15th Australasian Fluid Mechanics Conference, Sydney, Australia, Dec, 2004.

[5] H. F. Wang, Y. Zhou, C.K. Chan, W. O. Wong, and K.S. Lam, “Effect of initial conditions on interaction between a boundary layer and a wall-mounted finite-length-cylinder wake,” Physics of Fluids, vol. 18, no. 6, pp. 1-12, 2006.

[6] J. Y. Bae and G. S. Song, “The comparison of various turbulence models of the flow around a wall mounted square cylinder,” Journal of Korean Society of Marine Environment & Safety, vol. 26, no. 4, pp. 419-428, 2020.

[7] S. W. Lee and G. S. Song, “Study on resistance performance analysis using mesh generator in OpenFOAM,” Proceedings of the 2022 SNAK Annual Autumn Conference, 2022 (in Korean).

[8] P. G. Tucker, “Computation of unsteady internal flows: Fundamental methods with case studies,” Kluwer Academic Publishers, Norwell, Massachusetts, USA, 2001.

[9] E. E. Elhadi, X. Lei, and K. Wu, “Numerical simulation of 2D separated flow using two different turbulence models,” Journal of Applied Sciences, vol. 2, no. 12, pp. 1057-1062, 2002.

[10] C. S. Song and S. O. Park, “Numerical simulation of flow past a square cylinder using Partially-Averaged Navier–Stokes model,” Journal of Wind Engineering and Industrial Aerodynamics, vol. 97, no. 1, pp. 37-47, 2009.

[11] T. S. Fowler, F. D. Witherden, and S. S. Girimaji, “Partially-averaged Navier–Stokes simulations of turbulent flow past a square cylinder: Comparative assessment of statistics and coherent structures at different resolutions,” Physics of Fluids, vol. 32, 125106, 2020.

[12] J. Kim, “Experimental data for KCS resistance, sinkage, trim, and self-propulsion,” Numerical Ship Hydrodynamics, Lecture Notes in Applied and Computational Mechanics, vol. 94, Springer, 2021.